30th Congress of the International Council of the Aeronautical Sciences
DCC, Daejeon, Korea ; September 25-30, 2016

FLIGHT DYNAMIC STABILITY ANALYSIS OF A FLEXIBLE FLYING WING

Wang Libo*, Tang Chu*
*** The First Aircraft Institute of AVIC, Xi'an, Shaanxi, P.R. China 710089**

Keywords: *flight dynamics, stability analysis, flying wing, flexible aircraft*

Abstract

A method for flight dynamic stability analysis of flexible aircraft has been presented in this paper, which considers the rigid-body degrees of freedom as well as the elastic degrees of freedom of aircraft. The equations of motions of a flexible aircraft have been derived by using the energy function and Hamilton theory. The unsteady aerodynamics in time domain is computed by doublet lattice method and rational function approximation. The linear state-space model of the aircraft is then established based on the small disturbance theory, then the stability characteristics is computed by eigenvalue analysis of the characteristic matrix. For instance, the longitudinal stability analysis of a flying wing with large-aspect-ratio wings has been carried out by both the classic rigid flight dynamics and the method promoted. Results obtained by these two methods are compared, which indicate that the structural vibration of the flexible aircraft will interact with rigid-body flight dynamics, and it will have a great influence on the flight stability of the flying wing.

1 Introduction

The next generation long-range high-altitude ISR UAV – known as SensorCraft[1,2] is the research focus of aeronautics in recent years. A flying wing design with high-aspect-ratio wings is also a proposal for the SensorCraft. In order to satisfy the requirement of long endurance, high-aspect-ratio wings with advanced composite materials are commonly used because of their high lift-drag ratio and low structural weight. Therefore, the structures of the flying wing always have noticeable structural flexibility, and the frequency of the elastic vibration mode is very low. Besides, the flying wing layout always has a low pitching inertia, which leads a high frequency of the short-period mode. The flexible structural vibration modes will interact with rigid-body flight dynamics, which will have a great influence on the flight stability of the flying wing.

2 Theory

2.1 Equations of motions of the flexible aircraft

For a flexible aircraft, both the rigid body motion and the elastic deformation would be generated during flight. When establishing the equations of motion, the earth axes *OXYZ* is treated as the inertial reference frame. The origin *O* is an arbitrary point that fixed on the earth surface, and *OZ* directs vertically down. *OXY* is the local horizontal plane, *OX* points north, and *OY* points east. The mean axes system *oxyz*[3] is selected for the body reference frame. The origin of the mean axes system *o* coincides with the transient center of gravity of the aircraft, the *x* axis points from the nose to the tail along the fuselage axis, the *y* axis points to the right side perpendicular to the longitudinal symmetric plane of the aircraft, and the *z* axis is defined by the right-hand rule. The mean axes are body-fixed axes defined so that the relative linear and angular momenta due to elastic deformation are zero at every instant. Therefore, the inertial coupling between the rigid body degrees of freedom and the elastic degrees of freedom could be eliminated.

The location of the origin o in the earth axes is represented as $\boldsymbol{R}=[X \quad Y \quad Z]^{\mathrm{T}}$, and the Euler angle between the mean axes and the earth axes is $\boldsymbol{\theta}=[\phi \quad \theta \quad \psi]^{\mathrm{T}}$. The linear and angular velocity of the mean axes $oxyz$ relative to the earth axes is represented by $\boldsymbol{V}$ and $\boldsymbol{\omega}$. Meanwhile, the flexible structure is described by the finite elements method, the deformation of all the element grids is represented by $\boldsymbol{u}$. The kinetic energy and the potential energy can be written,

$$\begin{aligned} T &= \frac{1}{2} M \boldsymbol{V}^{\mathrm{T}} \boldsymbol{V} + \frac{1}{2} \boldsymbol{\omega}^{\mathrm{T}} \boldsymbol{I} \boldsymbol{\omega} + \frac{1}{2} \dot{\boldsymbol{u}}^{\mathrm{T}} \boldsymbol{m} \dot{\boldsymbol{u}} \\ U &= \frac{1}{2} \boldsymbol{u}^{\mathrm{T}} \boldsymbol{k} \boldsymbol{u} \end{aligned} \tag{1}$$

where, M is the total mass of the aircraft; $\boldsymbol{I}$ is the total inertia matrix of the aircraft, the effect of the structural deformation could be neglected if the elastic deformation is not large, and $\boldsymbol{I}$ could be treated as a constant matrix; $\boldsymbol{m}$ and $\boldsymbol{k}$ is the mass matrix and stiffness matrix of the finite element model.

The Lagrange function of the flexible aircraft can be written,

$$L = \frac{1}{2} M \boldsymbol{V}^{\mathrm{T}} \boldsymbol{V} + \frac{1}{2} \boldsymbol{\omega}^{\mathrm{T}} \boldsymbol{I} \boldsymbol{\omega} + \frac{1}{2} \dot{\boldsymbol{u}}^{\mathrm{T}} \boldsymbol{m} \dot{\boldsymbol{u}} - \frac{1}{2} \boldsymbol{u}^{\mathrm{T}} \boldsymbol{k} \boldsymbol{u} \tag{2}$$

Write the linear velocity as the components in mean axes, $\boldsymbol{V}=[U \quad V \quad W]^{\mathrm{T}}$, and the angular velocity $\boldsymbol{\omega}=[p \quad q \quad r]^{\mathrm{T}}$, referred as quasi-coordinates.

According to the Hamilton Principle, the equations of motion of the flexible aircraft in the mean axes system can be represented as

$$\begin{aligned} M\dot{\boldsymbol{V}} - M\tilde{\boldsymbol{\omega}}^{T} \boldsymbol{V} &= \boldsymbol{F}_{\mathrm{m}} \\ \boldsymbol{I}\dot{\boldsymbol{\omega}} + \tilde{\boldsymbol{\omega}} \boldsymbol{I} \boldsymbol{\omega} &= \boldsymbol{M}_{\mathrm{m}} \\ \boldsymbol{m}\ddot{\boldsymbol{u}} + \boldsymbol{b}\dot{\boldsymbol{u}} + \boldsymbol{k}\boldsymbol{u} &= \boldsymbol{Q}_{u} \end{aligned} \tag{3}$$

where, $\boldsymbol{F}_m$ and $\boldsymbol{M}_m$ are the generalized forces relative to the translational and rotational rigid body degrees of freedom, which equal to the resultant forces and moments in the means axes; $\boldsymbol{Q}_u$ is the generalized forces relative to the elastic deformation $\boldsymbol{u}$, which equals to the loads act on the grids of the finite elements. The loads including the gravity load $\boldsymbol{f}_G$, the aerodynamic load $\boldsymbol{f}_A$, and the thrust load $\boldsymbol{f}_T$, etc. The gravity loads $\boldsymbol{f}_G$ can be written,

$$\boldsymbol{f}_G = \boldsymbol{m} \begin{bmatrix} \boldsymbol{I}_3 \\ \boldsymbol{I}_3 \\ \vdots \end{bmatrix} \boldsymbol{g}_m \tag{4}$$

where, $\boldsymbol{I}_3$ is the 3×3 identity matrix. All the generalized forces can be written,

$$\begin{aligned} \boldsymbol{F}_{\mathrm{m}} &= \boldsymbol{\Phi}_{\mathrm{t}}^{\mathrm{T}} \boldsymbol{f}_{\mathrm{A}} + \boldsymbol{\Phi}_{\mathrm{t}}^{\mathrm{T}} \boldsymbol{f}_{\mathrm{T}} + M \boldsymbol{g}_{\mathrm{m}} \\ \boldsymbol{M}_{\mathrm{m}} &= \boldsymbol{\Phi}_{\mathrm{r}}^{\mathrm{T}} \boldsymbol{f}_{\mathrm{A}} + \boldsymbol{\Phi}_{\mathrm{r}}^{\mathrm{T}} \boldsymbol{f}_{\mathrm{T}} \\ \boldsymbol{Q}_{u} &= \boldsymbol{f}_{A} + \boldsymbol{f}_{T} + \boldsymbol{f}_{G} \end{aligned} \tag{5}$$

where, $\boldsymbol{g}_m$ is the acceleration vector of gravity in the mean axes, $\boldsymbol{\Phi}_t$ and $\boldsymbol{\Phi}_r$ are the mode matrix of translational and rotational rigid body motion.

The structural deformation $\boldsymbol{u}$ is assumed sufficiently small, so that it can be linearly superposed by several modes

$$\boldsymbol{u} = [\boldsymbol{\Phi}_e \quad \boldsymbol{\Phi}_c] \begin{bmatrix} \boldsymbol{q}_e \\ \boldsymbol{q}_c \end{bmatrix} \tag{6}$$

where, $\boldsymbol{\Phi}_e$ is the normal elastic mode matrix of free vibration of the structure, $\boldsymbol{\Phi}_c$ is the control surface deflection mode matrix, $\boldsymbol{q}_e$ and $\boldsymbol{q}_c$ are the generalized coordinates, respectively.

Substitute the results of equation (5) and (6) into equation (3), yields

$$\begin{aligned} & M\dot{\boldsymbol{V}} - M\tilde{\boldsymbol{\omega}}^{\mathrm{T}} \boldsymbol{V} = \boldsymbol{\Phi}_t^{\mathrm{T}} (\boldsymbol{f}_A + \boldsymbol{f}_T) + M\boldsymbol{g}_m \\ & \boldsymbol{I}\dot{\boldsymbol{\omega}} + \tilde{\boldsymbol{\omega}} \boldsymbol{I} \boldsymbol{\omega} = \boldsymbol{\Phi}_r^{\mathrm{T}} (\boldsymbol{f}_A + \boldsymbol{f}_T) \\ & \boldsymbol{M}_{ee} \ddot{\boldsymbol{q}}_e + \boldsymbol{B}_{ee} \dot{\boldsymbol{q}}_e + \boldsymbol{K}_{ee} \boldsymbol{q}_e = \\ & \boldsymbol{\Phi}_e^{\mathrm{T}} (\boldsymbol{f}_G + \boldsymbol{f}_A + \boldsymbol{f}_T) - \boldsymbol{M}_{ec} \ddot{\boldsymbol{q}}_c \end{aligned} \tag{7}$$

where, $\boldsymbol{M}_{ee} = \boldsymbol{\Phi}_e^{\mathrm{T}} \boldsymbol{m} \boldsymbol{\Phi}_e$, $\boldsymbol{B}_{ee} = \boldsymbol{\Phi}_e^{\mathrm{T}} \boldsymbol{b} \boldsymbol{\Phi}_e$ and $\boldsymbol{K}_{ee} = \boldsymbol{\Phi}_e^{\mathrm{T}} \boldsymbol{k} \boldsymbol{\Phi}_e$ are the elastic generalized mass, damping and stiffness matrix, respectively; $\boldsymbol{M}_{ec} = \boldsymbol{\Phi}_e^{\mathrm{T}} \boldsymbol{m} \boldsymbol{\Phi}_c$ is the coupling mass matrix between the control and the structural modes.

Combined with the kinematics equations of rigid degrees of freedom, the equations of motion of flexible aircraft can be written,

$$\begin{aligned} & M\dot{\boldsymbol{V}} - M\tilde{\boldsymbol{\omega}}^{\mathrm{T}} \boldsymbol{V} = \boldsymbol{\Phi}_t^{\mathrm{T}} (\boldsymbol{f}_A + \boldsymbol{f}_T) + M\boldsymbol{g}_m \\ & \boldsymbol{I}\dot{\boldsymbol{\omega}} + \tilde{\boldsymbol{\omega}} \boldsymbol{I} \boldsymbol{\omega} = \boldsymbol{\Phi}_r^{\mathrm{T}} (\boldsymbol{f}_A + \boldsymbol{f}_T) \\ & \boldsymbol{M}_{ee} \ddot{\boldsymbol{q}}_e + \boldsymbol{B}_{ee} \dot{\boldsymbol{q}}_e + \boldsymbol{K}_{ee} \boldsymbol{q}_e = \\ & \boldsymbol{\Phi}_e^{\mathrm{T}} (\boldsymbol{f}_G + \boldsymbol{f}_A + \boldsymbol{f}_T) - \boldsymbol{M}_{ec} \ddot{\boldsymbol{q}}_c \\ & \boldsymbol{V} = \boldsymbol{L}\dot{\boldsymbol{R}} \\ & \boldsymbol{\omega} = \boldsymbol{D}\dot{\boldsymbol{\theta}} \end{aligned} \tag{8}$$

where, $\boldsymbol{L}$ and $\boldsymbol{D}$ are the coefficient matrixes.

The small-disturbance theory[4] from conventional flight dynamics is still used to derive the linear equations of motion of the flexible aircraft. The reference steady state is taken to be symmetric rectilinear flight. The steady-state values are denoted by subscript 0 (for equilibrium) and changes from them by the prefix Δ. Thus for example

$$U = -V_\infty + \Delta U$$
$$W = W_0 + \Delta W \qquad (9)$$
$$q = q_0 + \Delta q$$

For the symmetric rectilinear flight situation with the true airspeed V_∞, there are $\boldsymbol{V}_0 = [-V_\infty \quad 0 \quad 0]^{\mathrm{T}}$, $\boldsymbol{\omega}_0 = \boldsymbol{0}$, $\boldsymbol{\theta}_0 = [0 \quad \pi \quad 0]^{\mathrm{T}}$, $\dot{\boldsymbol{V}}_0 = \dot{\boldsymbol{\omega}}_0 = \dot{\boldsymbol{\theta}}_0 = \boldsymbol{0}$, substitute the results into equation (8) yields

$$\begin{aligned}
& M\Delta\dot{\boldsymbol{V}} - M\tilde{\boldsymbol{V}}_0\Delta\boldsymbol{\omega} = \boldsymbol{\Phi}_t^{\mathrm{T}}(\Delta\boldsymbol{f}_G + \Delta\boldsymbol{f}_A + \Delta\boldsymbol{f}_T) \\
& \boldsymbol{I}\Delta\dot{\boldsymbol{\omega}} = \boldsymbol{\Phi}_r^{\mathrm{T}}(\Delta\boldsymbol{f}_G + \Delta\boldsymbol{f}_A + \Delta\boldsymbol{f}_T) \\
& \boldsymbol{M}_{ee}\ddot{\boldsymbol{q}}_e + \boldsymbol{B}_{ee}\dot{\boldsymbol{q}}_e + \boldsymbol{K}_{ee}\boldsymbol{q}_e = \\
& \boldsymbol{\Phi}_e^{\mathrm{T}}(\Delta\boldsymbol{f}_G + \Delta\boldsymbol{f}_A + \Delta\boldsymbol{f}_T) - \boldsymbol{M}_{ec}\ddot{\boldsymbol{q}}_c \\
& \Delta\dot{\boldsymbol{R}} = \boldsymbol{L}_0\Delta\boldsymbol{V} - \boldsymbol{L}_0\boldsymbol{T}\Delta\boldsymbol{\theta} \\
& \Delta\dot{\boldsymbol{\theta}} = \boldsymbol{D}_0\Delta\boldsymbol{\omega}
\end{aligned} \qquad (10)$$

where, $\boldsymbol{L}_0$, $\boldsymbol{D}_0$ and $\boldsymbol{T}$ are the coefficient matrixes.

2.2 Unsteady aerodynamics

The unsteady aerodynamics of the flexible aircraft in frequency domain is computed by the doublet lattice method, and then it is transformed into Laplace domain by aerodynamics rational function approximation approach[5,6]. The generalized aerodynamics in Laplace domain can be written

$$\boldsymbol{F}_A(\bar{s}) = q_D\boldsymbol{Q}(\bar{s})\boldsymbol{q} \qquad (11)$$

where, $\bar{s} = sc/2V_\infty$ is the nondimensional Laplace variable; s is the Laplace variable; c is the reference chord; $\boldsymbol{q}$ is generalized coordinates; $\boldsymbol{Q}(\bar{s})$ is the generalized aerodynamic influence coefficient matrix, and it could be attained by minimum-state approximation formula as

$$\boldsymbol{Q}_{\mathrm{ap}}(\bar{s}) = \boldsymbol{A}_0 + \boldsymbol{A}_1\bar{s} + \boldsymbol{A}_2\bar{s}^2 + \boldsymbol{D}(\boldsymbol{I}_r\bar{s} - \boldsymbol{R})^{-1}\boldsymbol{E}\bar{s} \qquad (12)$$

where, $\boldsymbol{A}_0$, $\boldsymbol{A}_1$, $\boldsymbol{A}_2$, $\boldsymbol{D}$, $\boldsymbol{E}$ are the approximation coefficients matrix; $\boldsymbol{R}$ is the aerodynamic root matrix, and the matrix order equals to the number of aerodynamic roots n_r; $\boldsymbol{I}_r$ is the $n_r \times n_r$ identity matrix. For the flexible aircraft, those matrixes can be written

$$\boldsymbol{A}_0 = \left[\begin{array}{ccc:c} \boldsymbol{A}_{0\mathrm{tt}} & \boldsymbol{A}_{0\mathrm{tr}} & \boldsymbol{A}_{0\mathrm{te}} & \boldsymbol{A}_{0\mathrm{tc}} \\ \boldsymbol{A}_{0\mathrm{rt}} & \boldsymbol{A}_{0\mathrm{rr}} & \boldsymbol{A}_{0\mathrm{re}} & \boldsymbol{A}_{0\mathrm{rc}} \\ \boldsymbol{A}_{0\mathrm{et}} & \boldsymbol{A}_{0\mathrm{er}} & \boldsymbol{A}_{0\mathrm{ee}} & \boldsymbol{A}_{0\mathrm{ec}} \end{array}\right]$$

$$\boldsymbol{A}_1 = \left[\begin{array}{ccc:c} \boldsymbol{A}_{1\mathrm{tt}} & \boldsymbol{A}_{1\mathrm{tr}} & \boldsymbol{A}_{1\mathrm{te}} & \boldsymbol{A}_{1\mathrm{tc}} \\ \boldsymbol{A}_{1\mathrm{rt}} & \boldsymbol{A}_{1\mathrm{rr}} & \boldsymbol{A}_{1\mathrm{re}} & \boldsymbol{A}_{1\mathrm{rc}} \\ \boldsymbol{A}_{1\mathrm{et}} & \boldsymbol{A}_{1\mathrm{er}} & \boldsymbol{A}_{1\mathrm{ee}} & \boldsymbol{A}_{1\mathrm{ec}} \end{array}\right]$$

$$\boldsymbol{A}_2 = \left[\begin{array}{ccc:c} \boldsymbol{A}_{2\mathrm{tt}} & \boldsymbol{A}_{2\mathrm{tr}} & \boldsymbol{A}_{2\mathrm{te}} & \boldsymbol{A}_{2\mathrm{tc}} \\ \boldsymbol{A}_{2\mathrm{rt}} & \boldsymbol{A}_{2\mathrm{rr}} & \boldsymbol{A}_{2\mathrm{re}} & \boldsymbol{A}_{2\mathrm{rc}} \\ \boldsymbol{A}_{2\mathrm{et}} & \boldsymbol{A}_{2\mathrm{er}} & \boldsymbol{A}_{2\mathrm{ee}} & \boldsymbol{A}_{2\mathrm{ec}} \end{array}\right] \qquad (13)$$

$$\boldsymbol{D} = \begin{bmatrix} \boldsymbol{D}_{\mathrm{t}} \\ \boldsymbol{D}_{\mathrm{r}} \\ \boldsymbol{D}_{\mathrm{e}} \end{bmatrix}$$

$$\boldsymbol{E} = \left[\begin{array}{ccc:c} \boldsymbol{E}_{\mathrm{t}} & \boldsymbol{E}_{\mathrm{r}} & \boldsymbol{E}_{\mathrm{e}} & \boldsymbol{E}_{\mathrm{c}} \end{array}\right]$$

$$\boldsymbol{q} = \begin{bmatrix} \boldsymbol{q}_{\mathrm{t}} \\ \boldsymbol{q}_{\mathrm{r}} \\ \boldsymbol{q}_{\mathrm{e}} \\ \boldsymbol{q}_{\mathrm{c}} \end{bmatrix}$$

where, the different subscript t, r, e, c means the translational and rotational modes of rigid body motion, the elastic mode, and the control mode, respectively. Use subscript s instead of subscript t, r, e (all the structural mode), there is

$$\begin{aligned}
& \boldsymbol{A}_0 = \left[\begin{array}{c:c} \boldsymbol{A}_{0\mathrm{ss}} & \boldsymbol{A}_{0\mathrm{sc}} \end{array}\right] \\
& \boldsymbol{A}_1 = \left[\begin{array}{c:c} \boldsymbol{A}_{1\mathrm{ss}} & \boldsymbol{A}_{1\mathrm{sc}} \end{array}\right] \\
& \boldsymbol{A}_2 = \left[\begin{array}{c:c} \boldsymbol{A}_{2\mathrm{ss}} & \boldsymbol{A}_{2\mathrm{sc}} \end{array}\right] \\
& \boldsymbol{E} = \left[\begin{array}{c:c} \boldsymbol{E}_{\mathrm{s}} & \boldsymbol{E}_{\mathrm{c}} \end{array}\right] \\
& \boldsymbol{q} = \left[\begin{array}{c} \boldsymbol{q}_{\mathrm{s}} \\ \hdashline \boldsymbol{q}_{\mathrm{c}} \end{array}\right]
\end{aligned} \qquad (14)$$

In this formulation, $\boldsymbol{A}_0$, $\boldsymbol{A}_1$, $\boldsymbol{A}_2$ are the coefficient matrixes represent the quasi-steady aerodynamic forces. The remnant terms are used to model the flow unsteadiness, whose effects can be modeled as a state-space realization,

$$\boldsymbol{x}_{\mathrm{a}} = (\boldsymbol{I}_{\mathrm{r}}\bar{s} - \boldsymbol{R})^{-1}[\boldsymbol{E}_{\mathrm{s}} \quad \boldsymbol{E}_{\mathrm{c}}]\left[\begin{array}{c} \boldsymbol{q}_{\mathrm{s}} \\ \hdashline \boldsymbol{q}_{\mathrm{c}} \end{array}\right]\bar{s} \qquad (15)$$

Written in time domain, there is

$$\dot{\boldsymbol{x}}_{\mathrm{a}} = \boldsymbol{E}_{\mathrm{s}}\dot{\boldsymbol{q}}_{\mathrm{s}} + \boldsymbol{E}_{\mathrm{c}}\dot{\boldsymbol{q}}_{\mathrm{c}} + \frac{2V_\infty}{c}\boldsymbol{R}\boldsymbol{x}_{\mathrm{a}} \tag{16}$$

Substituted equation (12), (14) and (15) into equation (11), yields

$$\begin{aligned} \Delta\boldsymbol{F}_A &= q_{\mathrm{D}}\boldsymbol{A}_{0\mathrm{ss}}\boldsymbol{q}_{\mathrm{s}} + q_{\mathrm{D}}\boldsymbol{A}_{0\mathrm{sc}}\boldsymbol{q}_{\mathrm{c}} + q_{\mathrm{D}}\frac{c}{2V_\infty}\boldsymbol{A}_{1\mathrm{ss}}\dot{\boldsymbol{q}}_{\mathrm{s}} + \\ & q_{\mathrm{D}}\frac{c}{2V_\infty}\boldsymbol{A}_{1\mathrm{sc}}\dot{\boldsymbol{q}}_{\mathrm{c}} + q_{\mathrm{D}}\frac{c^2}{4V_\infty^2}\boldsymbol{A}_{2\mathrm{ss}}\ddot{\boldsymbol{q}}_{\mathrm{s}} + \\ & q_{\mathrm{D}}\frac{c^2}{4V_\infty^2}\boldsymbol{A}_{2\mathrm{sc}}\ddot{\boldsymbol{q}}_{\mathrm{c}} + q_{\mathrm{D}}\boldsymbol{D}\boldsymbol{x}_{\mathrm{a}} \end{aligned} \tag{17}$$

2.3 Stability analysis of flexible aircraft

Considering the linear equation, and write in matrix format,

$$\begin{aligned} & \boldsymbol{M}_{\mathrm{s}}\ddot{\boldsymbol{q}}_{\mathrm{s}} + \boldsymbol{B}_{\mathrm{s}}\dot{\boldsymbol{q}}_{\mathrm{s}} + \boldsymbol{K}_{\mathrm{s}}\boldsymbol{q}_{\mathrm{s}} = \\ & q_{\mathrm{D}}\boldsymbol{A}_{0\mathrm{ss}}\boldsymbol{q}_{\mathrm{s}} + q_{\mathrm{D}}\boldsymbol{A}_{0\mathrm{sc}}\boldsymbol{q}_{\mathrm{c}} + q_{\mathrm{D}}\frac{c_{\mathrm{ref}}}{2V_\infty}\boldsymbol{A}_{1\mathrm{ss}}\dot{\boldsymbol{q}}_{\mathrm{s}} + \\ & q_{\mathrm{D}}\frac{c_{\mathrm{ref}}}{2V_\infty}\boldsymbol{A}_{1\mathrm{sc}}\dot{\boldsymbol{q}}_{\mathrm{c}} + q_{\mathrm{D}}\frac{c_{\mathrm{ref}}^2}{4V_\infty^2}\boldsymbol{A}_{2\mathrm{ss}}\ddot{\boldsymbol{q}}_{\mathrm{s}} + \\ & q_{\mathrm{D}}\frac{c_{\mathrm{ref}}^2}{4V_\infty^2}\boldsymbol{A}_{2\mathrm{sc}}\ddot{\boldsymbol{q}}_{\mathrm{c}} + q_{\mathrm{D}}\boldsymbol{D}\boldsymbol{x}_{\mathrm{a}} - \boldsymbol{M}_{\mathrm{sc}}\ddot{\boldsymbol{q}}_{\mathrm{c}} \end{aligned} \tag{18}$$

where,

$$\boldsymbol{M}_{\mathrm{s}} = \begin{bmatrix} M\boldsymbol{I}_3 & \boldsymbol{0}_{3\times3} & \boldsymbol{0}_{3\times n_e} \\ \boldsymbol{0}_{3\times3} & \boldsymbol{I} & \boldsymbol{0}_{3\times n_e} \\ \boldsymbol{0}_{n_e\times3} & \boldsymbol{0}_{n_e\times3} & \boldsymbol{M}_{\mathrm{ee}} \end{bmatrix}, \ddot{\boldsymbol{q}}_{\mathrm{s}} = \begin{bmatrix} \Delta\dot{\boldsymbol{V}} \\ \Delta\dot{\boldsymbol{\omega}} \\ \ddot{\boldsymbol{q}}_{\mathrm{e}} \end{bmatrix}$$

$$\boldsymbol{B}_{\mathrm{s}} = \begin{bmatrix} \boldsymbol{0}_{3\times3} & -M\tilde{\boldsymbol{V}}_0 & \boldsymbol{0}_{3\times n_e} \\ \boldsymbol{0}_{3\times3} & \boldsymbol{0}_{3\times3} & \boldsymbol{0}_{3\times n_e} \\ \boldsymbol{0}_{n_e\times3} & \boldsymbol{0}_{n_e\times3} & \boldsymbol{B}_{\mathrm{ee}} \end{bmatrix}, \dot{\boldsymbol{q}}_{\mathrm{s}} = \begin{bmatrix} \Delta\boldsymbol{V} \\ \Delta\boldsymbol{\omega} \\ \dot{\boldsymbol{q}}_{\mathrm{e}} \end{bmatrix}$$

$$\boldsymbol{K}_{\mathrm{s}} = \begin{bmatrix} \boldsymbol{0}_{3\times3} & -M\boldsymbol{T}_g & \boldsymbol{0}_{3\times n_e} \\ \boldsymbol{0}_{3\times3} & \boldsymbol{0}_{3\times3} & \boldsymbol{0}_{3\times n_e} \\ \boldsymbol{0}_{n_e\times3} & -\boldsymbol{M}_{\mathrm{eg}}\boldsymbol{T}_g & \boldsymbol{K}_{\mathrm{ee}} \end{bmatrix}, \boldsymbol{q}_{\mathrm{s}} = \begin{bmatrix} \Delta\boldsymbol{q}_{\mathrm{t}} \\ \Delta\boldsymbol{q}_{\mathrm{r}} \\ \boldsymbol{q}_{\mathrm{e}} \end{bmatrix}$$

$$\boldsymbol{M}_{\mathrm{sc}} = \begin{bmatrix} \boldsymbol{0}_3 \\ \boldsymbol{0}_3 \\ \boldsymbol{M}_{\mathrm{ec}} \end{bmatrix}$$

Yields,

$$\begin{aligned} \ddot{\boldsymbol{q}}_{\mathrm{s}} &= \bar{\boldsymbol{B}}_{\mathrm{s}}\dot{\boldsymbol{q}}_{\mathrm{s}} + \bar{\boldsymbol{K}}_{\mathrm{s}}\boldsymbol{q}_{\mathrm{s}} + \bar{\boldsymbol{K}}_{\mathrm{c}}\boldsymbol{q}_{\mathrm{c}} + \\ & \bar{\boldsymbol{B}}_{\mathrm{c}}\dot{\boldsymbol{q}}_{\mathrm{c}} + \bar{\boldsymbol{M}}_{\mathrm{c}}\ddot{\boldsymbol{q}}_{\mathrm{c}} + \bar{\boldsymbol{D}}\boldsymbol{x}_{\mathrm{a}} \end{aligned} \tag{19}$$

where,

$$\bar{\boldsymbol{M}} = (\boldsymbol{M}_{\mathrm{s}} - q_{\mathrm{D}}\frac{c_{\mathrm{ref}}^2}{4V_\infty^2}\boldsymbol{A}_{2\mathrm{ss}})^{-1}$$

$$\bar{\boldsymbol{M}}_{\mathrm{c}} = \bar{\boldsymbol{M}}(-\boldsymbol{M}_{\mathrm{sc}} + q_{\mathrm{D}}\frac{c_{\mathrm{ref}}^2}{4V_\infty^2}\boldsymbol{A}_{2\mathrm{sc}})$$

$$\bar{\boldsymbol{B}}_{\mathrm{s}} = -\bar{\boldsymbol{M}}(\boldsymbol{B}_{\mathrm{s}} - q_{\mathrm{D}}\frac{c_{\mathrm{ref}}}{2V_\infty}\boldsymbol{A}_{1\mathrm{ss}})$$

$$\bar{\boldsymbol{B}}_{\mathrm{c}} = q_{\mathrm{D}}\frac{c_{\mathrm{ref}}}{2V_\infty}\bar{\boldsymbol{M}}\boldsymbol{A}_{1\mathrm{sc}}$$

$$\bar{\boldsymbol{K}}_{\mathrm{s}} = -\bar{\boldsymbol{M}}(\boldsymbol{K}_{\mathrm{s}} - q_{\mathrm{D}}\boldsymbol{A}_{0\mathrm{ss}})$$

$$\bar{\boldsymbol{K}}_{\mathrm{c}} = q_{\mathrm{D}}\bar{\boldsymbol{M}}\boldsymbol{A}_{0\mathrm{sc}}$$

$$\bar{\boldsymbol{D}} = q_{\mathrm{D}}\bar{\boldsymbol{M}}\boldsymbol{D}$$

$$\bar{\boldsymbol{R}} = \frac{2V_\infty}{c_{\mathrm{ref}}}\boldsymbol{R}$$

Combining equation (16) and (19), write in state-space form as

$$\dot{\boldsymbol{x}} = \boldsymbol{A}\boldsymbol{x} + \boldsymbol{B}\boldsymbol{\eta} \tag{20}$$

where,

$$\boldsymbol{A} = \begin{bmatrix} \boldsymbol{0} & \boldsymbol{I}_{\mathrm{s}} & \boldsymbol{0} \\ \bar{\boldsymbol{K}}_{\mathrm{s}} & \bar{\boldsymbol{B}}_{\mathrm{s}} & \bar{\boldsymbol{D}} \\ \boldsymbol{0} & \boldsymbol{E}_{\mathrm{s}} & \bar{\boldsymbol{R}} \end{bmatrix}$$

$$\boldsymbol{B} = \begin{bmatrix} \boldsymbol{0} & \boldsymbol{0} & \boldsymbol{0} \\ \bar{\boldsymbol{K}}_{\mathrm{c}} & \bar{\boldsymbol{B}}_{\mathrm{c}} & \bar{\boldsymbol{M}}_{\mathrm{c}} \\ \boldsymbol{0} & \boldsymbol{E}_{\mathrm{c}} & \boldsymbol{0} \end{bmatrix}$$

$$\boldsymbol{x} = \begin{bmatrix} \boldsymbol{q}_{\mathrm{s}} \\ \dot{\boldsymbol{q}}_{\mathrm{s}} \\ \boldsymbol{x}_{\mathrm{a}} \end{bmatrix}$$

$$\boldsymbol{\eta} = \begin{bmatrix} \boldsymbol{q}_{\mathrm{c}} \\ \dot{\boldsymbol{q}}_{\mathrm{c}} \\ \ddot{\boldsymbol{q}}_{\mathrm{c}} \end{bmatrix}$$

As noted in Lyapunov stability theory, the linear system that defined in equation (20) is stable if all the real parts of the eigenvalues of characteristic matrix $\boldsymbol{A}$ are negative.

3 Numerical Example

3.1 Model

The longitudinal flight stability of a flexible flying wing has been analysis. The flying wing consists of the central blended wing body, large-aspect-ratio wings and the vertical tails locates at the wing tip, as shown in Fig. 1. The wing span of the flying wing is 4.800m, and the gross weight is 20kg. The static stability margin of the rigid aircraft is 16%.

According to the symmetric flight condition, the natural vibration characteristics of the flying wing structure have been analyzed. The result of structural dynamic characteristics is shown in Table 1.

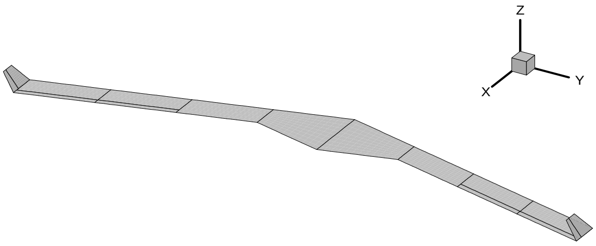

Fig. 1. Aerodynamic Layout of the Flying Wing

Table 1. The structural dynamic characteristics of the flying wing with symmetric boundary condition

	f / Hz	Mode
mode 1	0.0	Rigid body fore-aft motion
mode 2	0.0	Rigid body plunge
mode 3	0.0	Rigid body pitch
mode 4	3.67	Wing 1st bending
mode 5	20.32	Wing 2nd bending
mode 6	31.31	Wing 1st bending in plane with 1st torsion
mode 7	34.37	Wing 1st torsion
mode 8	39.61	Wing 3rd bending
mode 9	62.94	Outer wing 3rd bending
mode 10	86.13	Wing 4th bending
mode 11	101.71	Wing 2nd torsion

3.2 Longitudinal stability characteristics of rigid flying wing

The longitudinal aerodynamic derivatives of the rigid flying wing are listed in Table 2, and the longitudinal mode characteristics are calculated and illustrated in Fig. 2 and Fig. 3, including the root locus of phugoid mode and short-period mode. The result shows that the damping and frequency of the phugoid mode decreases with the increase of the velocity. However, the damping and frequency of the short-period keep increasing with the increase of the velocity.

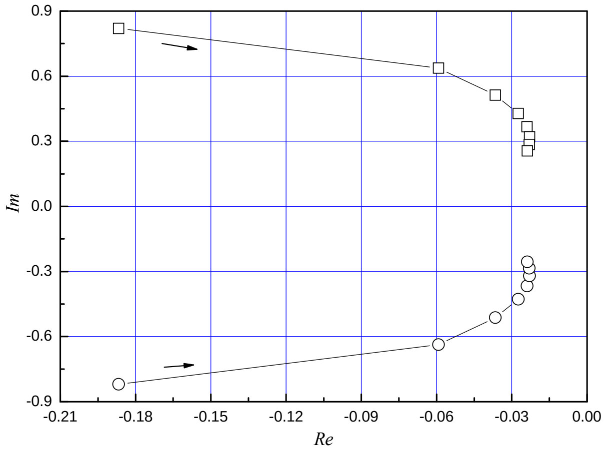

Fig. 2 Root locus of phugoid mode of the rigid flying wing (V=15m/s~50m/s)

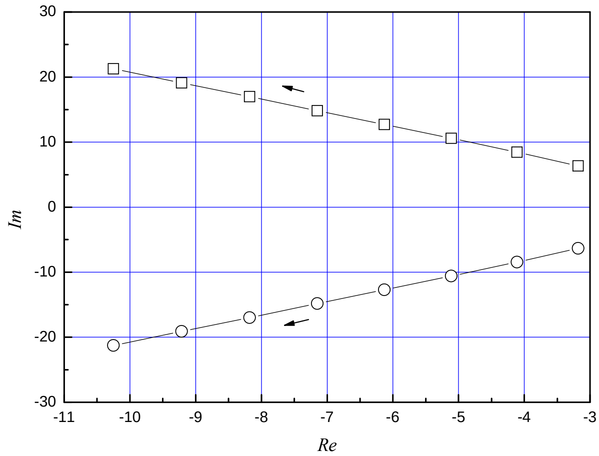

Fig. 3 Root locus of short-period mode of the rigid flying wing (V=15m/s~50m/s)

3.3 Longitudinal stability characteristics of elastic flying wing

The longitudinal stability characteristics of the elastic flying wing are analyzed by using the method proposed in this paper. Three rigid body degrees of freedom, eight elastic degrees of freedom that mentioned above and one aerodynamic root are all considered when establishing the state-space model of the elastic flying wing. The root locus relative to the velocity is shown in Fig. 4. The result indicates that, with the increase of velocity, the root locus of the short-period mode cross the imaginary axis at a velocity of 26.1m/s (more detail of the short-period root locus is shown in Fig. 5). Which means the system is unstable when V>26.1m/s.

By Comparing the root locus of phugoid and short-period mode of rigid and elastic flying wings, the result shows that the characteristics of short-period mode are influenced by the coupling effects of the rigid body degrees of motion and the elastic degrees of motion.

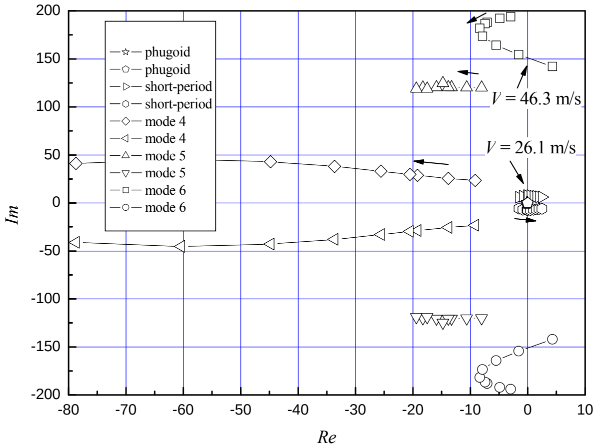

Figure 4 Root locus of the flexible flying wing (V=15m/s~50m/s)

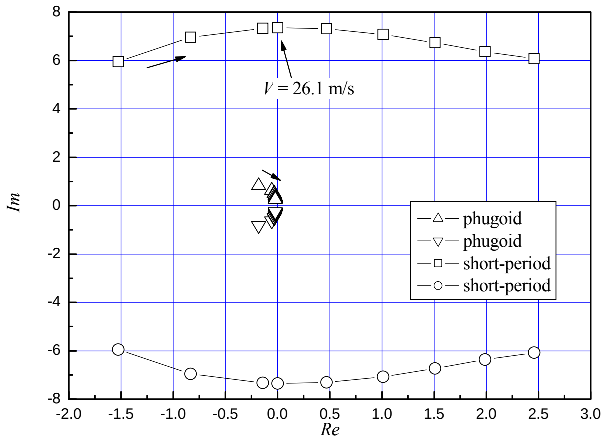

Figure 5 Details of the short-period mode and phugoid root locus of the flexible flying wing (V=15m/s~50m/s)

3.4 Time domain response analysis

As both of the state-space models of the rigid and elastic flying wing have been developed in the former sections, let the initial disturbance of the angle of attack is 1.0 degree, the time domain response of the flying wing has been analyzed with different velocities. Table 3 shows the response of trajectory, angle of attack Δα, forward velocity Δu, pitch rate Δq and pitch angle Δθ, when the system is stable (V_∞=20m/s), critical stable (V_∞=26.1) and unstable (V_∞=30m/s).

4 Conclusion

A method for flight dynamic stability analysis of flexible aircraft has been presented in this paper, which considers the rigid-body degrees of freedom as well as the elastic degrees of freedom of aircraft.

From the numerical example, the longitudinal stability analysis of a flying wing with large-aspect-ratio wings has been carried out by both the rigid flight dynamics and the method presented. Results obtained by these two methods are compared, which indicate that the structural vibration of the flexible aircraft will interact with rigid-body flight dynamics, and it will have a great influence on the flight stability of the flying wing.

Table 2. The longitudinal aerodynamic derivatives of the rigid flying wing

V_∞	15m/s	20m/s	25m/s	30m/s	35m/s	40m/s	45m/s	50m/s
α/deg	12.90	7.25	4.64	3.22	2.36	1.80	1.42	1.15
δ_e/deg	-15.51	-8.72	-5.58	-3.87	-2.84	-2.17	-1.72	-1.39
C_{L0}	1.0314	0.5903	0.3796	0.2641	0.1942	0.1487	0.1175	0.0952
C_{D0}	0.3461	0.0851	0.0408	0.0248	0.0180	0.0147	0.0129	0.0119
$C_{D\alpha}$	0.2136	0.1223	0.0787	0.0548	0.0404	0.0309	0.0245	0.0199
$C_{L\alpha}$	5.2947	5.2981	5.3024	5.3076	5.3139	5.3211	5.3294	5.3387
$C_{m\alpha}$	-0.8033	-0.8039	-0.8046	-0.8055	-0.8066	-0.8078	-0.8093	-0.8109
C_{Lq}	7.7595	7.7641	7.7700	7.7772	7.7858	7.7957	7.8071	7.8197
C_{mq}	-6.0396	-6.0430	-6.0473	-6.0526	-6.0589	-6.0662	-6.0746	-6.0839
$C_{D\delta e}$	0.0000	0.0000	0.0000	0.0000	0.0000	0.0000	0.0000	0.0000
$C_{L\delta e}$	0.4926	0.4930	0.4932	0.4936	0.4942	0.4946	0.4954	0.4960
$C_{m\delta e}$	-0.6680	-0.6684	-0.6684	-0.6694	-0.6700	-0.6727	-0.6716	-0.6726
$C_{m\dot{\alpha}}$	-0.6040	-0.6043	-0.6047	-0.6053	-0.6059	-0.6066	-0.6075	-0.6084

Table 2. Time domain response of the flying wing with different velocities

V_∞=20.0 m/s	V_∞=26.1 m/s	V_∞=30.0 m/s

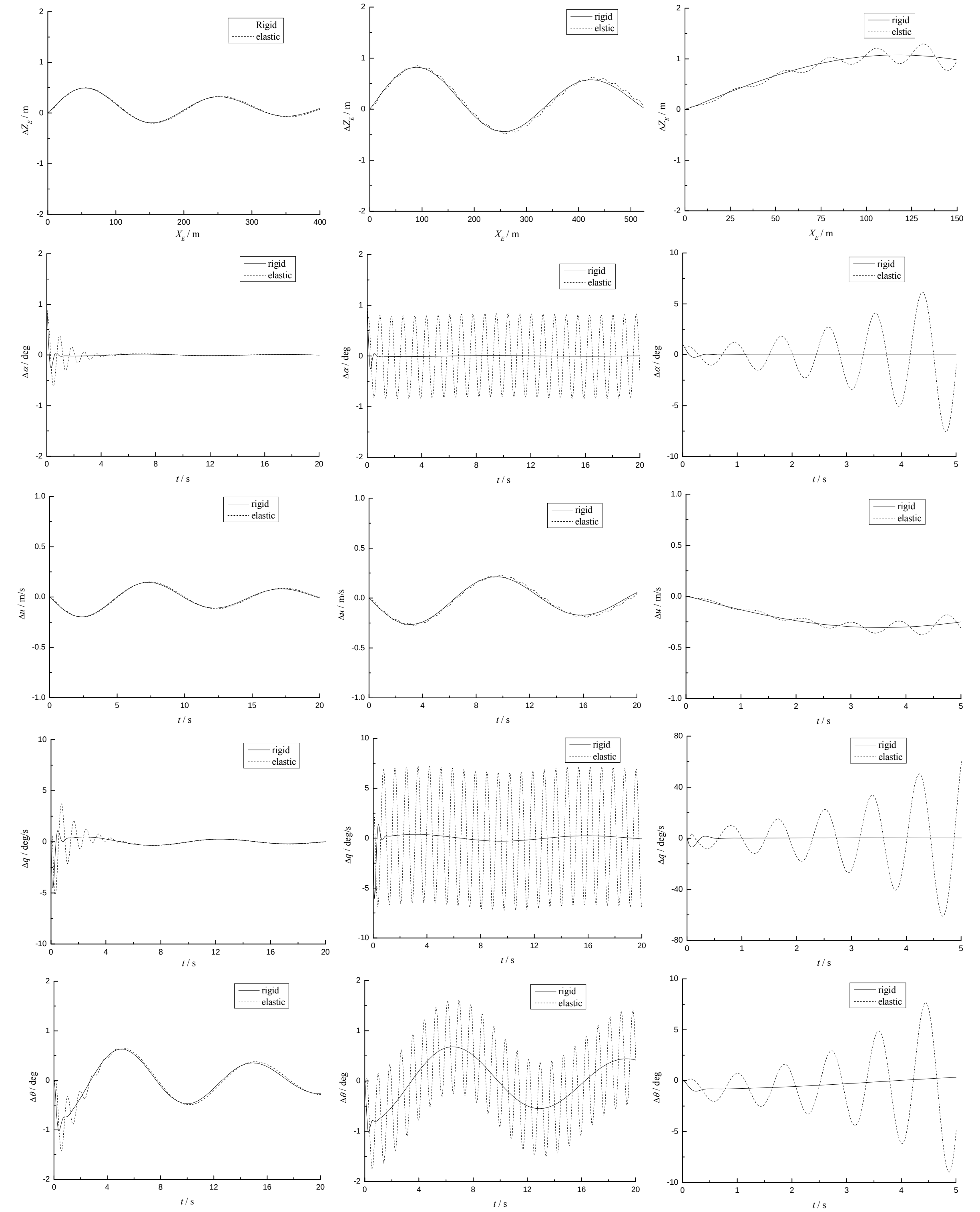

References

[1] Bartley-Cho J D, Henderson J A. Design and analysis of HiLDA/AEI aeroelastic wind tunnel model[R]. AIAA 2008-7191, 2008

[2] Patil M J. Nonlinear aeroelastic analysis of Joined-Wing aircraft[R]. AIAA 2003-1487, 2003

[3] Swain R L, Fullman D G. A unique formulation of elastic airplane longitudinal equations of motion[R]. AIAA 77-403, 1977

[4] Bernard E. Dynamics of atmospheric flight. Dover Publications. INC., 2005

[5] ROGER K L. Airplane math modeling methods for active control design[R]. In Structural Aspects of Active controls, AGARD CP-228,1997:4.1-4.11

[6] KAPEL M. Design for active and passive flutter suppression and gust alleviation[R]. NASA R-3482, 1980

Contact Author Email Address

volleyball458@163.com

Copyright Statement